ELSEVIER

Journal of Chromatography B, 706 (1998) 73–82

JOURNAL OF CHROMATOGRAPHY B

Capillary zone electrophoresis in normal or reverse polarity separation modes for the analysis of hydroxy acid oligomers in neutral phosphate buffer

Christian Braud*, Rémy Devarieux, Audrey Atlan, Cathy Ducos, Michel Vert

C.R.B.A., URA CNRS 1465, Faculté de Pharmacie, Université de Montpellier 1, 15 Avenue Charles Flahault, 34060 Montpellier, France

Abstract

Capillary zone electrophoresis (CZE) with neutral phosphate buffer as the background electrolyte was used to analyse water-soluble oligomers obtained by polycondensation of racemic lactic acid. Two CZE separation modes were tested. The first mode was based on normal separation (injection at the anodic side) using a fused-silica capillary. Eight peaks were observed within a 60-min migration time range. They were ascribed to dimer and higher water-soluble oligomers. Peaks from dimer to tetramer were split due to sensitivity for the fine structures at the level of the distribution of chiral lactic acid moieties in oligomer chains. The second mode was based on reverse separation (injection at the cathodic side) using a fused-silica capillary modified by adsorption of a polycation on its inner wall. Under these conditions, oligomers were rapidly separated without peak splitting. Considering the forces which are involved in CZE, data were plotted as a function of $1/t$ scale, according to the equation $[\text{signal}]=f((-1)^k/t)$ where $k=0$ and $k=1$ for normal and reverse separation modes, respectively. Such a plot allowed direct comparison between the various runs after a simple translation along the $1/t$ axis, regardless of the separation mode and the variation of electroosmotic flow. The second separation mode allowed separation of 3-hydroxybutyric acid and 6-hydroxyhexanoic acid oligomers. For the former series of oligomers, a side reaction generating crotyl bonds was observed due to the high sensitivity of CZE. It was shown that separation was governed by the ratio charge/mass of the oligoesters whatever their structure. © 1998 Elsevier Science B.V.

Keywords: Lactic acid; 3-Hydroxybutyric acid; 6-Hydroxyhexanoic acid

1. Introduction

The hydrolytic degradation of aliphatic polyesters is an increasingly attractive area of polymer science, mostly because these polymers have a potential as bioresorbable materials for therapeutic applications in surgery and in pharmacology, as well as for plastic waste management and biorecycling [1–3]. A complete description of the degradation pathways requires the assessment of the formed polymeric chains of various lengths varying from high molecular mass to small oligomers, including the ultimate degradation by-products. Different analytical techniques have to be used because of their inherent limits or because of changes in the physico-chemical properties of the analytes with ageing.

Size-exclusion chromatography (SEC) and high-performance liquid chromatography (HPLC) have been widely used to investigate the hydrolytic degradation of polyesters derived from lactic acid enantiomers (PLA), glycolic acid (PGA), hydroxy-3-butyric acid ((P(3-HB)), ϵ-caprolactone (PCL), etc. Both

*Corresponding author.

0378-4347/98/$19.00
PII S0378-4347(97)00468-4

techniques appeared efficient in organic solvents, in water, as well as in mixtures of water with organic solvents. Hydrolytic degradation of aliphatic polyesters occurs generally in water. Moreover, polyester hydrolysis leads to shorter chains which bear ionogenic groups, namely carboxyl, at one or at both chain ends, depending on the chain structure. This particularity makes high-performance capillary electrophoresis (HPCE) and, more specifically, capillary zone electrophoresis (CZE) of interest for monitoring the final stages of abiotic and biomediated degradation.

With regard to the CZE separation, it must be pointed out that the literature only contains information concerning the analysis of non-degradable oligomers bearing charged end-groups. They migrate less rapidly when the ratio charge/mass is decreased [4–8]. In the case of DL-lactic acid oligomers (OLA50) obtained by condensation of the hydroxy acid, CZE was successfully used in 100 m*M* borate buffer at pH 8.9 (BBS) with normal separation (injection at the anodic side; denoted as normal mode in the following) [9]. In order to avoid this slightly basic medium which affected the stability of oligomers [10], neutral 50 m*M* phosphate buffer at pH 6.8 buffer (PBS) was preferred for the second stage. Furthermore, the use of a fused-capillary coated with a polycation allowed us to show that the nine smaller PLA oligomers were soluble in water at neutral pH [11]. However, these data were collected after reverse separation (injection at the cathodic side; named reverse mode in the following) and were not easily comparable to the ones obtained using the normal mode.

In this paper, we report on the different CZE techniques for the separation of oligomers of hydroxy acids (lactic acid, 3-hydroxybutyric acid, 6-hydroxyhexanoic acid) by using fused-silica capillaries running with PBS as the background electrolyte. After revisiting the CZE theory as applied to the cases of normal and reverse mode, we used a data representation based on the plot of the signal as a function of 1/[migration time] or −1/[migration time] for injection at the positive or negative inlet, respectively. This mode of representation appeared to readily facilitate the comparison of data between different runs when using the same analytical parameters (electric field, background electrolyte, temperature) for a given mode of injection. Moreover, the high separation efficiency of CZE allowed us to reveal fine structures of oligomers as a diastereoisomeric effect in the case of OLA or dehydration reaction in the case of degradation products of P(3-HB).

2. Experimental

2.1. Materials

DL-, L-, D- and *meso*-lactide, and ϵ-caprolactone were obtained from Purac (Gorinchem, Netherlands) and Aldrich (Gillingham, UK) respectively. They were used without further purification. Bacterial P(3-HB) was obtained from Solvay (Paris, France). All other chemicals used were of analytical grade.

A 1000 ml solution of 0.1 *M* borate buffer at pH 8.9 (BBS) was obtained by neutralising 6.184 g boric acid (Roth, Karlruhe, Germany) with 1 *M* NaOH up to pH 8.9; a 1000 ml solution of 0.05 *M* phosphate buffer at pH 6.8 (PBS) was obtained by dissolving 4 g $NaH_2PO_4 \cdot 2H_2O$ (Prolabo, Paris, France) and 8.72 g $Na_2HPO_4 \cdot 12H_2O$ (Prolabo) in pure water.

2.2. Synthesis

2.2.1. Lactic acid oligomers

Lactic acid oligomers were obtained by mild condensation (8 h at 90°C) of commercial aqueous solution of lactic acid as described elsewhere [11].

2.2.2. Sodium lactyllactate

A 500 mg quantity of lactide (DL-, L-, D- or meso-lactate) was dispersed in PBS (100 cm^3). As the reaction proceeded, the initial pH value was maintained by adding 1 *M* NaOH. After 3 h at room temperature, no lactide crystals remained in the medium. The buffered solution was then filtered through a 0.22 μm Millipore filter for sterilisation. The resulting sodium lactyllactate was stored in solution.

2.2.3. 3-Hydroxybutyric acid oligomers

Oligomers were produced by partial degradation of P(3-HB) as described previously [12]. Typically,

P(3-HB) (4 g) was introduced in a 500 ml round bottom flask equipped with a cooling device. The polymer was dissolved in 1,2-dichloroethane using heat and stirring. After dissolution, *p*-toluenesulfonic acid monohydrate (0.4 g) and water (0.9 ml) were added. The clear solution was refluxed for 10 h. The organic solution was cooled and transferred to a 1-l separation funnel. PBS (200 ml) was added and the funnel was shacken for 3 min. It was then allowed to rest for 10 to 30 min until a clear separation of the two solvents was obtained. The aqueous phase was finally collected. A second extraction of the organic phase was performed with fresh PBS (200 ml). Both extracts were mixed and then filtered through a 0.22 μm filter.

2.2.4. 6-Hydroxyhexanoic oligomers

ε-Caprolactone (10 g) was dissolved in water (20 ml). The solution was stirred at 80°C for 2 days in order to open the lactone ring. Then, polycondensation was performed by heating for 2 h at 80°C under vacuum. The temperature was then raised stepwise from 120 to 150°C for 6 h under vacuum.

2.3. Methods

2.3.1. CZE

Data were collected using a P/ACE 5000 Beckman instrument equipped with UV absorbance detection at 200 nm. Fused-silica capillaries (50 or 75 μm I.D.) were used either with normal or reverse mode. In the case of normal mode, the capillary was rinsed stepwise before each run, first for 2 min with 1 *M* HCl, then for 1 min with water and for 2 min with 1 *M* NaOH, and finally for 2 min with PBS. In some experiments, the final step was replaced with a 2-min rinse using BBS and a 2-min rinse with PBS. In the case of reverse mode, the capillary was conditioned at the start of each day by the following rinses: first for 30 min with 1 *M* HCl, then for 1 min with water and for 30 min with 1 *M* NaOH, and finally for 5 min with PBS. Furthermore, the capillary was rinsed before each run, first for 5 min with 0.1% DEAE dextran in PBS, then for 1 min with water and finally for 3 min with PBS. Separations were performed at 25°C with an applied voltage of 30 or 20 kV. After the last run of the day, the capillary was rinsed for 30 min with 1 *M* NaOH, followed by 5 min with water before being stored wet. All the oligomers (ca. 0.3% or less) were initially dissolved in PBS. Samples were injected in the capillary by the hydrostatic pressure method (5 s and 10 s for 75 μm I.D. and 50 μm I.D. capillaries, respectively). In all experiments, one drop of an aqueous solution of benzyl alcohol (5 g l^{-1}) was added to the analyte (4 ml).

2.3.2. Mathematical treatment of data

The matrix UA=$f(t)$, where UA and t are the UV absorption signal and the migration time, respectively, was transformed into UA=$f((-1)^k/t)$ (where $k=0$ and $k=1$ for normal and reverse modes, respectively) by using Sigmaplot 2.0 for Windows which allowed a direct view of the transformation.

3. Results and discussion

For a better understanding of our results, it is necessary to refer to the CZE driving force parameters in normal and reverse modes. From a general viewpoint, CZE is governed by the effective velocity of the ionic component i and the electroosmotic flow (EO flow) due to counter ions neutralising the fixed charges borne by the capillary wall, whatever their sign. The EO flow, which is the driving force of CZE separation, can be estimated by introducing a neutral marker [13]. In the case of lactic acid separation, benzyl alcohol has been successfully employed [9,11].

In the case of a classical CZE separation (normal mode) with a fused-silica capillary, Eqs. (1) and (2) are currently used [14]:

$$v_i = v_{i(net)} - v_{EO} = \frac{L_D}{t_i} - \frac{L_D}{t_{EO}} \quad (1)$$

$$\mu_i = \frac{L_D.L_T}{V}.\left[\frac{1}{t_i} - \frac{1}{t_{EO}}\right] \quad (2)$$

with: v_i the effective velocity of ionic component i, $v_{i(net)}$, the observed velocity (in cm s^{-1}) of ionic component i giving a peak at t_i (in s), v_{EO}, the observed velocity (in cm s^{-1}) of the EO marker giving a peak at t_{EO} (in s), μ_i, the effective electrophoretic mobility (in cm^2 V^{-1} s^{-1}) of ionic component i, V, the applied voltage (in V), L_D, the length

from the inlet of the capillary to the detection window (in cm), L_T, the total length of the capillary (in cm).

Eq. (2) actually gives the norm of the effective electrophoretic mobility vector $\vec{\mu}_i$ which is the vector sum defined by:

$$\vec{\mu}_i = \vec{\mu}_i(\text{net}) - \vec{\mu}_{EO} \quad (3)$$

where $\vec{\mu}_{i(net)}$ and $\vec{\mu}_{EO}$ are the observed mobility vectors of the ionic component i and of the EO marker, respectively. Eq. (3) can be considered as a general representation of CZE phenomena regardless of the site of injection (anode or cathode) and the sense of EO.

If one defines a unitary vector $\vec{u}$ oriented from anode to cathode, Eq. (3) can be rewritten as:

$$\vec{\mu}_i = \|\vec{\mu}_i\|.\vec{u} = (\|\vec{\mu}_{i(net)}\| - \|\vec{\mu}_{EO}\|).(-1)^k.\vec{u} \quad (4)$$

where $k=0$ and $k=1$ for normal and reverse modes respectively. Thus, the norm of takes the general form:

$$\|\vec{\mu}_i\| = (-1)^k.\frac{L_D.L_T}{V}.\left[\frac{1}{t_i} - \frac{1}{t_{EO}}\right] \quad (5)$$

3.1. CZE separation of OLA50 in PBS

Condensation of DL-lactic acid yields a whole series of oligomers [9,11]. The high conductivity of PBS imposes a lower voltage which increases the time of analysis in normal mode [9]. Moreover, migration time values of analytes greatly depend on the conditioning of the capillary. This dependency was observed for several capillaries.

The behaviour of one of them was studied in more detail (Table 1). The newly set-up capillary was successively rinsed with 1 *M* HCl and 1 *M* NaOH. In order to check the efficiency of the capillary, the test suggested by Beckman for fused-silica capillaries running in a borate buffer was performed and gave accurate separations. Then, when using PBS as the running buffer, a progressive shift of the EO marker from 7.01 to 9.41 min was observed (Table 1; runs 1–4). This variation affected the migration time values of the peaks assigned to oligomers. The lower velocity of the EO marker did not permit the detection of the dimer in the 60 min analysis range for runs 2–4.

Rinsing the capillary first with BBS and then with PBS and running the separation in PBS allowed us to recover EO values in the range of 7.16–7.30 min (Table 1; runs 5–8) that permit the separation of oligomers up to the dimer. In the absence of the preliminary rinse with BBS (Table 1; runs 9–12), the migration time of the EO marker was increased from run to run. In conclusion, rinsing with borate buffer dramatically affects the CZE separation performances made in PBS. Such rinsing appears necessary to obtain reproducible electropherograms. While this behaviour remains unexplained, it must be noted that for a given oligomer, the t_i values allow the calculation of constant effective electrophoretic mobility values (Table 1), thus showing that the separation in PBS is governed by CZE phenomena.

An example of an electropherogram obtained in PBS is given in Fig. 1. Peaks were assigned using the protocol precedently described [11]. In the 60 min separation range, dimer (peak 2) and higher water-soluble oligomers (peaks 3–8) can be detected. It is interesting to note that the dimer, trimer and tetramer peaks were split. This point will be developed below by comparison of electrophoretic properties of OLA50, L-lactic acid oligomers (OLA100) and lactyllactate with different structures.

CZE separation of lactic acid oligomer was also performed in PBS by using the same capillary which was previously rinsed with a solution of a polyca-

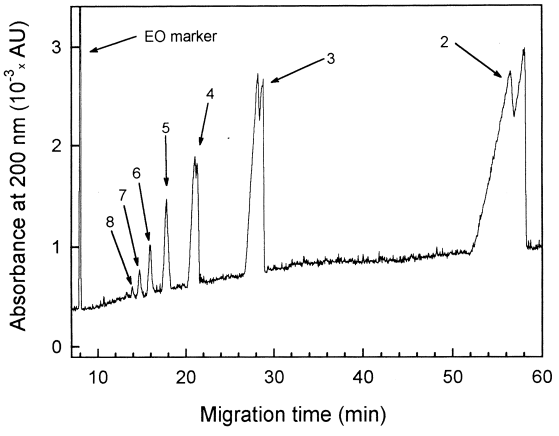

Fig. 1. Electropherogram of OLA50 (run #12 of Table 1) [Fused-silica capillary ($\phi_{int}=75$ μm, $L_T=56.5$ cm, $L_D=49.9$ cm); background electrolyte: PBS; Tre=25°C; $V=+20$ kV; normal mode].

Table 1
Migration time (t)[a] and calculated effective electrophoretic mobility (μ_i)[b] of peaks observed during separation of oligomers of OLA50 in PBS

Run[b]	Rinsing procedure	EO		Heptamer		Hexamer		Pentamer		Tetramer		Trimer		Dimer	
		t_{EO}	$10^4\mu_{EO}$	t_i	$10^4\mu_i$	t_i	$10^4\mu_i$	t_i	$10^4\mu_i$	t_i	$10^4\mu_i$	t_i	$10^4\mu_i$	t_i	$10^4\mu_i$
1	PBS	7.01	3.35	11.57	−1.32	12.29	−1.44	13.37	−1.59	15.16	−1.80	18.72	−2.10	29.98	−2.57
2	PBS	8.10	2.90	14.98	−1.33	16.23	−1.45	18.18	−1.61	21.71	−1.82	29.71	−2.11		
3	PBS	9.09	2.58	18.78	−1.33	20.80	−1.45	24.10	−1.61	30.56	−1.82	47.91	−2.09		
4	PBS	9.41	2.50	20.15	−1.33	22.49	−1.45	26.46	−1.61	34.18	−1.81	56.46	−2.08		
5	BBS+PBS	7.16	3.28	11.82	−1.29	12.61	−1.42	13.80	−1.58	15.78	−1.79	19.70	−2.09	32.02	−2.55
6	BBS+PBS	7.22	3.25	12.13	−1.32	12.94	−1.44	14.12	−1.59	16.12	−1.80	20.17	−2.09	32.43	−2.53
7	BBS+PBS	7.26	3.24	12.29	−1.33	13.04	−1.44	14.27	−1.59	16.36	−1.80	20.49	−2.09	33.57	−2.54
8	BBS+PBS	7.30	3.22	12.32	−1.31	13.17	−1.43	14.40	−1.59	16.52	−1.80	20.83	−2.09	34.50	−2.54
9	PBS	7.44	3.16	12.75	−1.31	13.56	−1.42	14.97	−1.59	17.33	−1.80	22.35	−2.11	40.39	−2.57
10	PBS	7.41	3.17	12.64	−1.31	13.51	−1.43	14.80	−1.58	17.08	−1.80	21.97	−2.10	39.09	−2.57
11	PBS	7.78	3.02	13.84	−1.32	14.90	−1.44	16.57	−1.60	19.43	−1.81	25.58	−2.10	54.20	−2.59
12	PBS	8.04	2.92	14.70	−1.32	15.92	−1.45	18.04	−1.62	21.01	−1.80	29.30	−2.12	56.00	−2.50
Mean[c]					−1.32		−1.44		−1.60		−1.80		−2.10		−2.55
[d]					−1.33		−1.45		−1.60		−1.79		−2.07		−2.49

Fused-silica capillary; $L_T = 56.5$ cm; $L_D = 49.9$ cm; Tre = 25°C; $V = +20$ kV (normal mode).
[a] Deduced from the middle of the width of the peak at half height (t in min).
[b] μ_i (in $cm^2\ V^{-1}\ s^{-1}$) calculated using Eq. (5).
[c] Mean values of calculated intrinsic electrophoretic mobility from run 1–12.
[d] Mean values (5 runs) of calculated intrinsic electrophoretic mobility deduced from CZE in PBS with the fused-silica capillary coated with DEAE dextran [Same capillary; Tre = 25°C; $V = -20$ kV (reverse mode)].

tion, DEAE dextran, as reported previously [11]. The polycation strongly adsorbed on the inner wall of the capillary reversing the electroosmotic flow as already noted with other polycations [15,16]. Thus, the separation can be performed after injection at the cathodic inlet (reverse mode). The reproducibility of migration time was better (3%) and all the oligomers, even lactic acid at 5 min (peak 1), were separated within 10 min (Fig. 2). However, peaks were not split in contrast to what was observed in Fig. 1. The use of the same capillary with the same background electrolyte at a constant temperature and voltage (i.e. the same electric field) allowed us to compare effective electrophoretic mobility values calculated using Eq. (5). Values from reverse injection are in accordance with the one obtained from the normal mode (Table 1), thus showing that mobility does not depend on EO characteristics imposed by the inner surface of the capillary.

The shapes of the curves $[AU]=f(t)$ of Figs. 1 and 2 cannot be directly compared due to different CZE separation modes. It must be noted that the graphical plot ($[signal]=f(t)$) does not directly offer a visual representation of CZE driving forces represented by Eq. (5) since mobility is an inverse function of the migration time. Thus plots of $[signal]=f((-1)^k/t)$ were considered. Data have been redrawn by plotting $[AU]=f(1/t)$ and $[AU]=f(-1/t)$ respectively (Fig. 3). The two resulting fingerprints can now easily be compared after a simple translation along the X-axis which is now a mobility axis. It offers a graphical representation which visualises the velocities of the different components and which is a direct application of Eq. (5).

Moreover, for a series of runs in a given injection mode with a given capillary, the representation $[AU]=f(1/t)$ or $[AU]=f(-1/t)$ improves the visual comparison of CZE data from run-to-run, which is a general problem when t_{EO} is not constant [17]. As an example, Fig. 4 shows a schematic view of peak data collected in Table 1 (runs 5–8) using the two representations. The left column of Fig. 4 reflects the time-variation of the classical electropherogram ($[AU]=f(t)$) from run-to-run, spacing between peaks depending on the EO value. Conversely, the representation using $1/t$ for the same data improves the visual comparison where spacing between similar peaks is proportional to the difference of their mobility.

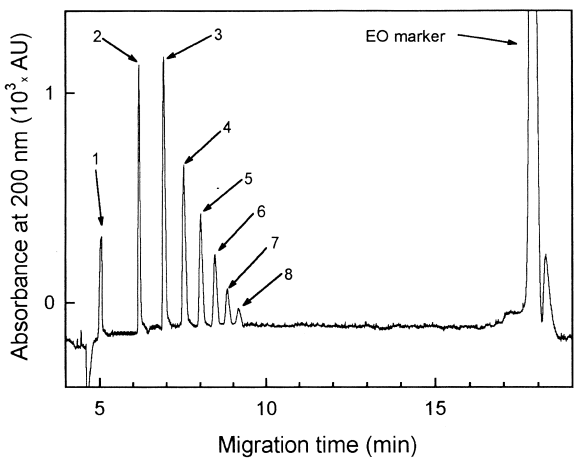

Fig. 2. Electropherogram of OLA50 [Fused-silica capillary coated with DEAE Dextran ($\phi_{int}=75$ μm, $L_T=56.5$ cm, $L_D=49.9$ cm); background electrolyte: PBS; Tre=25°C; $V=-20$ kV; reverse mode].

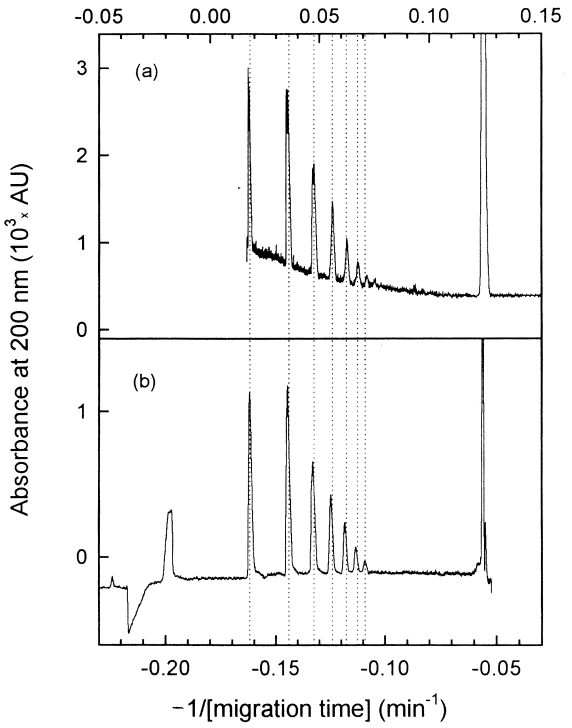

Fig. 3. Plot of signals of Fig. 1 and Fig. 2 as a function of $1/t$ (a) and $-1/t$ (b) respectively.

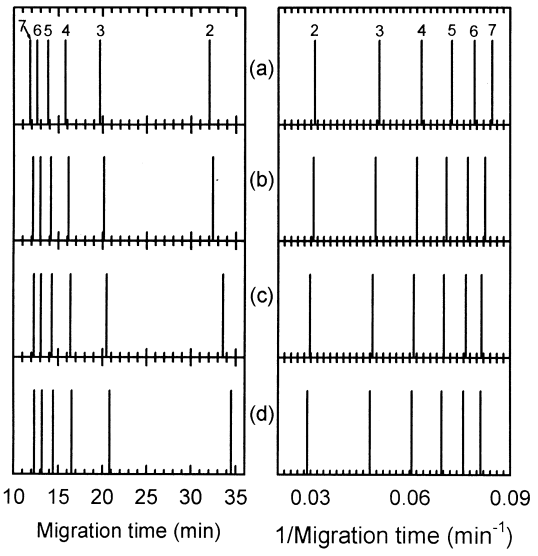

Fig. 4. Data of Table 1 ((a): run 5; (b): run 6; (c): run 7 and (d): run 8) plotted as a function of migration time (left column) and 1/[migration time] (right column) [The vertical bars represent the location of the peaks of dimer to heptamer, and not their magnitudes in the electropherogram].

3.2. Diastereoisomeric dependence of CZE peaks for OLA50 in PBS

While separation with the normal mode in PBS needs long time analysis due to the low electroosmosis, the lagging effect which is generated allows the peaks of dimer, trimer and tetramer to split. A similar separation using OLA100 does not show such a behaviour. This agrees well with the chiral structure of OLA100 oligomers. Condensation of L-lactic acid leads to a unique distribution of L-lactic acid moieties (noted -L-) in the condensate. In contrast, condensation of DL-lactic acid gives a more complex distribution of moieties where L- and D-moieties (noted -D-) can be more or less randomly distributed along the polymer chain. Until now, ^{1}H NMR was the only method to detect such steric differences [18]. The splitting of peaks on Fig. 1 can thus be ascribed to differences between -L- and -D-linkages which generate various oligomeric stereoisomers.

As far as the dimer peak is concerned, this assignment was confirmed by considering the CZE behaviour of the four lactyllactate diastereoisomers (HO-L-L-COO$^-$, HO-L-D-COO$^-$, HO-D-L-COO$^-$ and HO-D-D-COO$^-$). These lactyllactic acid compounds were obtained by hydrolysis of the different lactides in PBS as previously reported for racemic lactide [9]. Each of the L-lactide and D-lactide is formed from two identical lactic acid molecules, L- and D-, respectively. DL-Lactide is the 50/50 mixture of L- and D-lactide. Only *meso*-lactide is formed from one molecule of L- and one molecule of D-lactic acid [19]. While *meso*-lactide leads to lactyllactate with hetero-linkages (-D-L- and -L-D-), all the other lactides give lactyllactate with homo-linkage (-L-L- and -D-D-).

Lactyllactates of L-, D-, DL- and *meso*-lactide, gave only one CZE peak (Fig. 5a), thus showing that under the conditions used no enantiomeric separation occurs in agreement with the absence of chiral selector [13,14,20]. Mixtures of lactyllactate diastereoisomers with homo and hetero structures, as in the case of Fig. 5b and 5c, led to a partially split

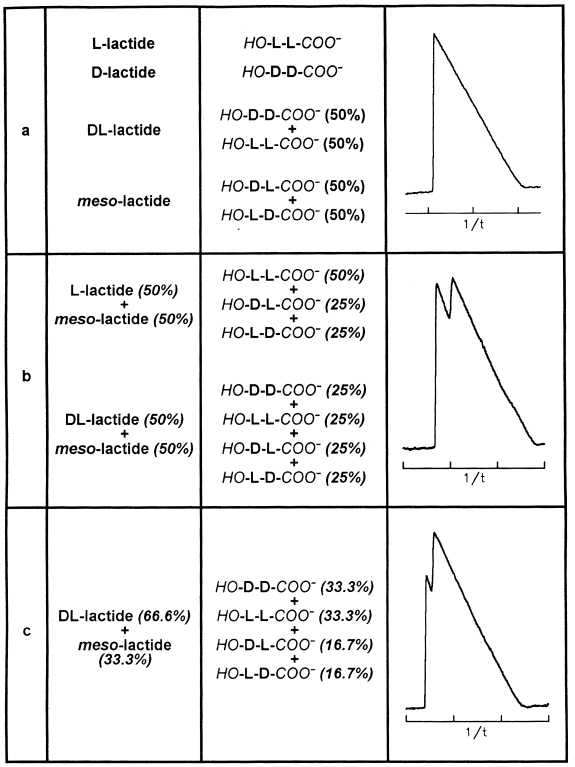

Fig. 5. Dimer signal recorded at 200 nm (arbitrary units) of mixtures of isomers of lactyllactate obtained by ring-opening of different lactide mixtures.

signal which is a composition of two CZE peaks with close mobility. Moreover, by comparing the magnitude of these peaks, the higher mobility peak (on the left side) can be assigned to HO-L-D-COO^- and HO-D-L-COO^- isomers while the lower mobility one (on the right side) is assigned to HO-D-D-COO^- and HO-L-L-COO^- ones. Such diastereoisomeric separation was also observed for diastereoisomer derivatives of α-amino acids by CZE [21].

3.3. Generalisation to other oligomers of hydroxy acids

While PLA received attention in the biomedical field, today it is becoming a candidate in the environmental polyester family where P(3-HB) and PCL are the more studied systems. As PLA, these polymers can give water-soluble oligomers that can be studied by CZE.

Cleavage of high molecular mass chains of P(3-HB) was achieved in a homogenous medium obtained by dissolving the polyester in 1,2-dichloroethane at 70°C, followed by the addition of a small volume of water and of *p*-toluenesulfonic acid (*p*-TSA), the latter being used to catalyse the ester cleavage according to a synthetic route described by Vanlautem [22]. The solution was refluxed for up to 10 h. Then, the organic phase was extracted by using PBS.

The aqueous extract was analysed by CZE using the reverse mode previously described (Fig. 6). A series of peaks was observed between −0.30 and −0.15 min^{-1}. The peak at −0.27 min^{-1} was assigned to *p*-TSA. It interferes with the peak of 3-hydroxybutyric acid (noted 1 in Fig. 6). Peak 1′ was identified as crotonic acid. These peak assignments were made by co-injection of the pure compounds assumed to be present. Peaks 2 to 7 were assigned to oligomers having the same moiety as P(3-HB) (O(3-HB)) with a degree of polymerisation (*i*) varying from 2 to 7 by comparison with the behaviour of lactic acid oligomers. As *i* increased, the charge/weight ratio decreased, as well as the mobility of the component. On the left side of peaks 2, 3 and 4, highly absorbing species (O′(3-HB)) were observed which were assigned to oligomers bearing a C=C bond at the non-carboxylic terminus (Scheme 1) on the basis of our previous work on O(3-HB) polycondensates [11]. It must be noted that a low amount of O′(3-HB) oligomers can be easily detected due to their high absorption characteristics.

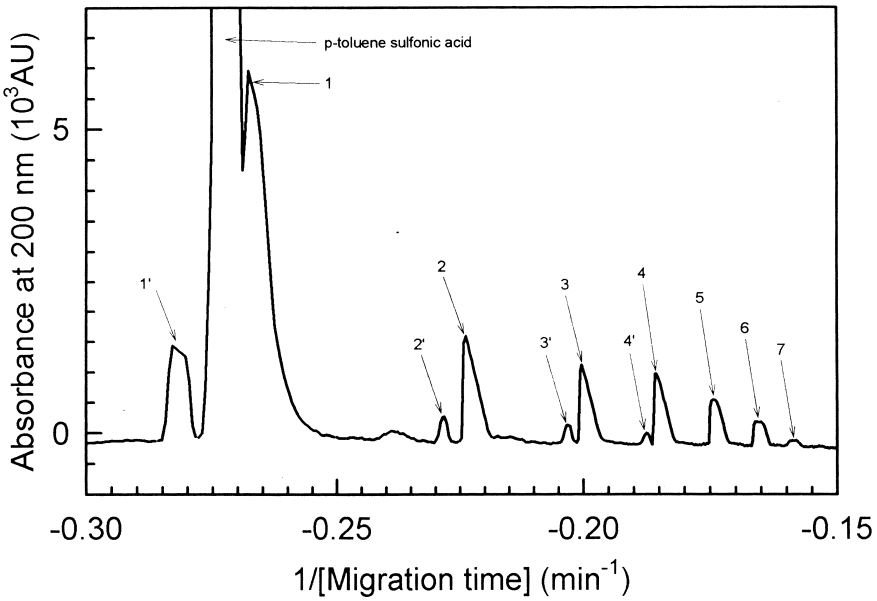

Fig. 6. Electropherogram of oligomers of 3-hydroxybutyric acid [Fused-silica capillary coated with DEAE dextran (ϕ_{int} = 75 μm, L_T = 56.5 cm, L_D = 49.9 cm); background electrolyte: PBS; Tre = 25°C; V = −30 kV; reverse mode; for peak assignment see the text].

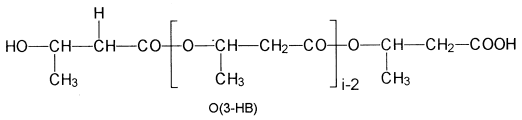

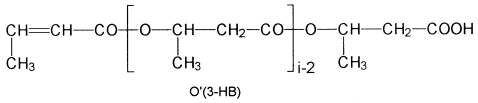

Scheme 1.

The C=C groups which are conjugated with the C=O groups absorb about 400 times more than the carboxylic chromophores at 200 nm [23]. Thus the electropherogram recorded at 200 nm does not reflect the respective amounts of each series of oligomers. Under the selected hydrolysis conditions, the O′(3-HB) oligomers constitute a minor population formed during the slow hydrolytic cleavage of P(3-HB) chains.

Oligomers derived from PCL were synthesised by polycondensation of 6-hydroxyhexanoic acid which was obtained from hydrolysis of ε-caprolactone. The water-soluble oligomers (OHH) were extracted with PBS from dichloromethane solutions of the polycondensate. CZE analysis gives a fingerprint where only four peaks were detected (Fig. 7). The peak at -0.24 min^{-1} was assigned to sodium 6-hydroxyhexanoate.

The plot of effective electrophoretic mobility of the different oligomers observed using CZE with the reverse mode running in PBS as a function of the molar mass gives a master curve (Fig. 8). This behaviour shows that the structure of the oligomer plays a minor role as compared to its mass, thus showing that the ratio charge to mass is the main factor driving the separation. This variation confirms the assignment of higher water-soluble oligomers in each series.

4. Conclusion

Separation of oligomers of lactic acid has been successfully performed in a fused- silica capillary filled with PBS using the normal and reverse modes. In the case of normal mode, reproducibility in terms of migration time is poor and requires a prior rinse of the capillary with BBS. This separation procedure allows the detection of fine structure at the level of

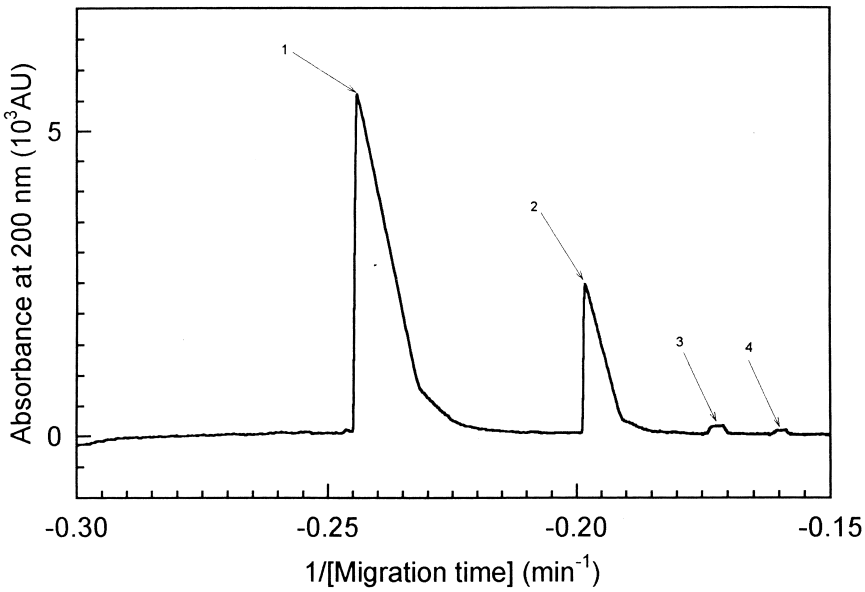

Fig. 7. Electropherogram of oligomers of 6-hydroxyhexanoic acid [Fused-silica capillary coated with DEAE dextran ($\phi_{int}=75$ μm, $L_T=56.5$ cm, $L_D=49.9$ cm); background electrolyte: PBS; Tre=25°C; $V=-30$ kV; reverse mode; for peak assignment see the text].

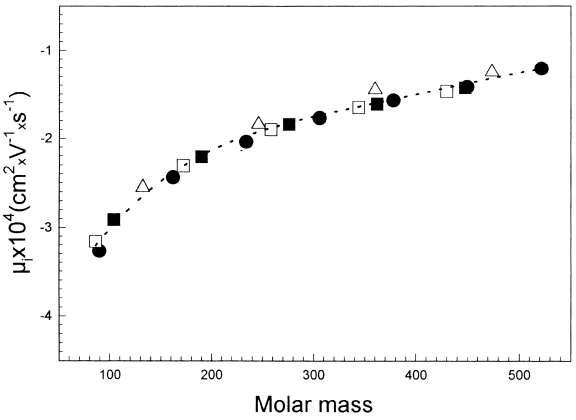

Fig. 8. Effective electrophoretic mobility of oligomers of hydroxy acids (●: OLA 100; ■: O(3-HB); □: O′(3-HB); △: OHH) [Fused-silica capillary coated with DEAE Dextran (ϕ_{int} = 50 μm, L_T = 57.1 cm, L_D = 50.5 cm); background electrolyte: PBS; Tre = 25°C; V = −30 kV; reverse mode].

the distribution of lactic acid moieties in polymer chains.

Better separations are obtained using a DEAE dextran coated fused-silica capillary in the reverse injection mode. This procedure was applied to oligomers of P(3-HB) and PCL. In the case of P(3-HB) oligomers, the sensitivity of CZE allowed the detection of a side reaction leading to oligomers bearing a C=C bond at the non-carboxylic acid end.

The data recorded using this procedure show that the main driving force of the separation is the ratio charge/mass whatever the structure of the oligomers.

The variation of migration times from run to run allows us to propose a new representation of data by plotting [signal] = $f((-1)^k/t)$, which corresponds to the basic concept of mobility in CZE. This concept is exemplified by the aliphatic oligoester separations presented herein.

References

[1] M. Vert, J. Feijen, A. Albertsson, G. Scott, E. Chiellini, Biodegradable Polymers and Plastics, The Royal Society of Chemistry, Cambridge, 1992.
[2] Y. Doi, K. Fukuda, Biodegradable Plastics and Polymers, Elsevier, Amsterdam, 1994.
[3] G. Scott, D. Gilead, Degradable Polymers – Principles and Applications Chapman and Hall, London, 1995.
[4] W. Nashabeh, Z. El Rassi, J. Chromatogr. 514 (1990) 57.
[5] J. Liu, O. Shirota, M. Novotny, J. Chromatogr. 559 (1991) 223.
[6] J.T. Smith, Z. El Rassi, J. High Resolut. Chromatogr. 15 (1992) 573.
[7] P.J. Oefner, C. Chiesa, Glycobiology 4 (1994) 397.
[8] J. Bullock, J. Chromatogr. 645 (1993) 169.
[9] C. Vidil, C. Braud, H. Garreau, M. Vert, J. Chromatogr. A 711 (1995) 323.
[10] J. Mauduit, Ph. D.Thesis. (Rouen, France) 1991.
[11] C. Braud, R. Devarieux, H. Garreau, M. Vert, J. Environ. Polym. Degrad. 4 (1996) 135.
[12] A. Atlan, C. Braud, M. Vert, J. Environ. Polym. Degrad. 5 (1997) 243.
[13] F. Foret, L. Krivankova, P. Bocek, Capillary Zone Electrophoresis, VCH, Weinheim, 1993.
[14] R. Kuhn, S. Hoffsteter-Kuhn, Capillary Electrophoresis: Principles and Practice, Springer-Verlag, Berlin, 1993.
[15] N. Cohen, E. Grushka, J. Cap. Elec. 1 (1994) 112.
[16] G. Schomburg, D. Belder, M. Gilges, S. Motsch, J. Cap. Elec. 1 (1994) 219.
[17] J. Yang, S. Rose, D.S. Hage, J. Chromatogr. A 735 (1996) 209.
[18] J.L. Espartero, I. Rasshkov, S.M. Li, N. Manolova, M. Vert, Macromolecules 29 (1996) 3535.
[19] C.H. Holten, Lactic Acid – Properties and Chemistry of Lactic Acid and Derivatives, Verlag Chemie, Wheinheim, 1971, Ch. XI.
[20] S.F.Y. Li, Capillary Electrophoresis: Principles, Practice and Applications, Elsevier Science Publishers, Amsterdam, 1992.
[21] W. Schützner, G. Caponecchi, S. Fanali, A. Rizzi, E. Kenndler, Electrophoresis 15 (1994) 769.
[22] N. Vanlautem, European Patent No. 0 043 620 B1 (1981)
[23] D.W. McLellan, P.J. Halling, J. Chromatogr. 445 (1988) 251.